Electron-Transfer Reactions of Iron, Ruthenium, and Osmium Bipyridine and Phenanthroline Complexes at Polymer/Solution Interfaces

C. R. Leidner and Royce W. Murray*

Contribution from the Kenan Laboratories of Chemistry, University of North Carolina, Chapel Hill, North Carolina 27514. *Received July 5, 1983*

Abstract: The kinetics of the thermodynamically unfavorable oxidations of a series of iron, ruthenium, and osmium bipyridine and phenanthroline complexes in acetonitrile solutions by poly[$(bpy)_2Os(vpy)_2]^{3+}$-coated rotated Pt disk electrodes are reported. Measurement of these back-reaction rates is made possible by the electrode-driven regeneration of Os(III) in the polymer film and by convective removal of the oxidized complex. The variation of the kinetic rates with reaction free energies in the complex series quantitatively agrees with the Marcus outer-sphere cross-reaction relation, and the extrapolated self-exchange rate-constant products $k_{11}k_{22}$ agree with those derived from literature values for homogeneous solution self exchanges. The analysis of the kinetic data involved demonstration that the electron transfers occur exclusively with the outermost monolayer of Os sites in the poly$[(bpy)_2Os(vpy)_2]^{3+}$ film, a circumstance that probably contributes to the simplicity of the electron-transfer reaction energetics.

Electron-transfer reactions at the interface between two fluid, nonmetallic media are an important event in diverse areas of chemistry, including among others photodriven reactions at micelle and vesicle surfaces,[1] electron transport across biological[2] and man-made membranes,[3] and electron transfer between contacting polymers as in bilayer electrodes[4] and xerography.[5] Such reactions tend to be very rapid or coupled to other complex steps, and there is a paucity of quantitative data on their rates. In the case where one of the phases is a polymer and the other a solvent, the problem is further complicated by uncertainty about the actual dimensions of the polymer/solution interface, as illustrated by the classical study by Whitesides et al.[6] on oxidized poly(ethylene) surfaces. Quantitative information on the rates and locations of electron transfers at polymer/solution interfaces should thus have some general usefulness and is the object of this paper.

Our work on redox polymers[4a,7] has evolved a series of ruthenium, iron, and osmium polypyridine complex monomers that can be electrochemically polymerized to form remarkably uniform, pinhole free, electroactive, 60–10 000-Å films on electrodes. By adjustment of electrode potential, the electrode can act as an electron acceptor to drive the polymer film from, say, an Os(II) to Os(III) oxidation state. The Os(III) state of the film can in turn be used to oxidize metal complexes dissolved in the solution contacting the polymer film, an electron-transfer mediation scheme represented by reaction 1. The film of poly$[(bpy)_2Os(vpy)_2]^{2+}$ is prepared on a Pt electrode by reduction of the monomer $[(bpy)_2Os(vpy)_2]^{2+}$, bpy and vpy being 2,2′-bipyridine and 4-vinylpyridine, respectively.

Table I. Metal Complexes Employed

compound	$E_s^{\circ\prime}$, V vs. SSCE[a]
catalyst, poly-$[(bpy)_2Os(vpy)_2]^{2+/3+}$	0.72_0 ($=E_c^{\circ\prime}$)
I, $[(3,4,7,8\text{-}Me_4(phen))_3Fe](PF_6)_2$	0.81_2
II, $[(4,4'\text{-}Me_2(bpy))_3Fe](PF_6)_2$	0.89_0
III, $[(4,7\text{-}Me_2(phen))_3Fe](PF_6)_2$	0.89_8
IV, $[(4,4'\text{-}Ph_2(bpy))_3Fe](PF_6)_2$	0.96_0
V, $[(4\text{-}Me(phen))_3Fe](PF_6)_2$	0.98_0
VI, $[(4,7\text{-}Ph_2(phen))_3Fe](PF_6)_2$	0.98_8
VII, $[(5,6\text{-}Me_2(phen))_3Fe](PF_6)_2$	0.99_2
VIII, $[(5\text{-}Me(phen))_3Fe](PF_6)_2$	1.02_8
IX, $[(bpy)_3Fe](PF_6)_2$	1.04_0
X, $[(phen)_3Fe](PF_6)_2$	1.05_8
XI, $[(3,4,7,8\text{-}Me_4(phen))_3Ru](PF_6)_2$	1.01_0
XII, $[(4,4'\text{-}Me_2(bpy))_3Ru](PF_6)_2$	1.09_0
XIII, $[(bpy)_2Ru(3,4,7,8\text{-}Me_4(phen))](PF_6)_2$	1.18_0
XIV, $[(bpy)_3Ru](PF_6)_2$	1.25_5
XV, $[(bpy)_2OsCl_2]$	-0.06_1
XVI, $[(5\text{-}Cl(phen))_3Os](PF_6)_2$	0.90_1
XVII, $[(5\text{-}NO_2(phen))_3Os](PF_6)_2$	0.90_8
XVIII, $[(3,4,7,8\text{-}Me_4(phen))_3Os](PF_6)_2$	0.57_0

[a] Average of $E^{\circ\prime}$ in cyclic voltammetry and $E_{1/2}$ in rotated-disk voltammetry.

The electron-transfer reaction of eq 1 results in a flow of current since the electrode acts to regenerate the Os(III) states. Conditions resulting in control of the current by the rate of eq 1 would permit a measurement of k_{12}, since the necessary interpretive theory is available.[8,9] The currents measured on rotated-disk electrodes for substrate complexes $[L_3M]^{2+}$ with formal potentials $E_s^{\circ\prime}$ *less positive* than the Os(II/III) potential $E_c^{\circ\prime}$ of the polymer (i.e., the electron-transfer reaction in eq 1 has a favorable free energy change) are limited by other processes;[9] k_{12} is too large to measure. We have found on the other hand[9] that if $E_s^{\circ\prime}$ is *more positive* than $E_c^{\circ\prime}$, the currents can be controlled by the much slower rate of eq 1, and k_{12} is measurable. This situation is highly advantageous, as it allows (i) quantitative evaluation of electron-transfer rates at a polymer/solution interface, (ii) study of how such rates k_{12} vary with the free energy change $\Delta E^\circ = E_s^{\circ\prime} - E_c^{\circ\prime}$ by using a series of substrate complexes $[L_3M]^{2+}$ with differing $E_s^{\circ\prime}$, (iii) direct evaluation of the electron-transfer reaction rate in its thermodynamically unfavorable, back-reaction direction (which

(1) Fendler, J. H. "Catalysis in Micellar and Macromolecular Systems"; Academic Press: New York, 1975.
(2) (a) Jortner, J. *Biochim. Biophys. Acta* **1980**, *594*, 193. (b) Loach, P. A.; Runquist, J. A.; Kong, J. L. Y.; Dannhauser, K. G.; Spears, K. G. *Adv. Chem. Ser.* **1981**, *No. 201*.
(3) Lehn, J.-M. In "Physical Chemistry of Transmembrane Ion Motions"; Elsevier: Amsterdam, 1983; p 181.
(4) (a) Abruna, H. D.; Denisevich, P.; Umana, M.; Meyer, T. J.; Murray, R. W. *J. Am. Chem. Soc.* **1981**, *103*, 1. (b) Denisevich, P.; Willman, K. W.; Murray, R. W. *Ibid.* **1981**, *103*, 4727. (c) Willman, K. W.; Murray, R. W. *J. Electroanal. Chem.* **1982**, *133*, 211. (d) Schneider, J. R.; Murray, R. W. *Anal. Chem.* **1982**, *54*, 1508. (e) Pickup, P. G.; Leidner, C. R.; Denisevich, P.; Murray, R. W. *J. Electroanal. Chem.*, in press.
(5) Mort, J.; Pai, D. M. "Photoconductivity and Related Phenomona"; Elsevier: Amsterdam, 1976.
(6) (a) Rasmussen, J. R.; Stedronsky, E. R.; Whitesides, G. M. *J. Am. Chem. Soc.* **1977**, *99*, 4736. (b) Rasmussen, J. R.; Bergbreiter, D. E.; Whitesides, G. M. *Ibid.* **1977**, *99*, 4746.
(7) (a) Denisevich, P.; Abruna, H. D.; Leidner, C. R.; Meyer, T. J.; Murray, R. W. *Inorg. Chem.* **1982**, *21*, 2153. (b) Calvert, J. M.; Schmehl, R. H.; Sullivan, B. P.; Facci, J. S.; Meyer, T. J.; Murray, R. W. *Ibid.* **1983**, *22*, 2151.
(8) (a) Andrieux, C. P.; Dumas-Bouchiat, J. M.; Saveant, J.-M. *J. Electroanal. Chem.* **1982**, *131*, 1. (b) Andrieux, C. P.; Saveant, J.-M. *Ibid.* **1982**, *134*, 163; (c) *Ibid.* **1982**, *142*, 1.
(9) Ikeda, T.; Leidner, C. R.; Murray, R. W. *J. Electroanal. Chem.* **1982**, *138*, 343.

0002-7863/84/1506-1606$01.50/0

$$\text{Pt/poly}[(\text{bpy})_2\text{Os}(\text{vpy})_2]^{3+} + L_3M^{2+} \xrightleftharpoons[k_{12}]{-e^-} \text{Pt/poly}[(\text{bpy})_2\text{Os}(\text{vpy})_2]^{2+} + L_3M^{3+} \quad (1)$$

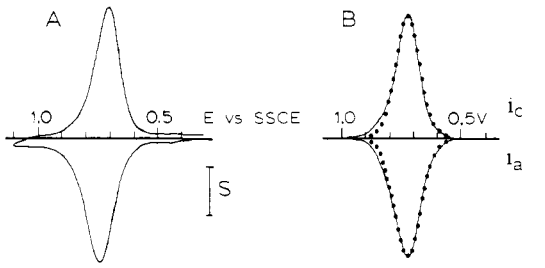

Figure 1. (A) Cyclic voltammetric response of a Pt/poly-$[(bpy)_2Os(vpy)_2]^{2+/3+}$ electrode with $\Gamma_T = 7.6 \times 10^{-9}$ mol/cm^2 in 0.1 M Et_4NClO_4/CH_3CN at 100 mV/s. $S = 196$ μA/cm^2. (B) Linear-sweep voltammograms (—) of the same electrode obtained with a microcomputer electrochemical setup at 50 mV/s and theoretical voltammograms (●●●) generated by using $G_a = -1.45$ and $G_c = -0.95$ with a 2% impurity peak.

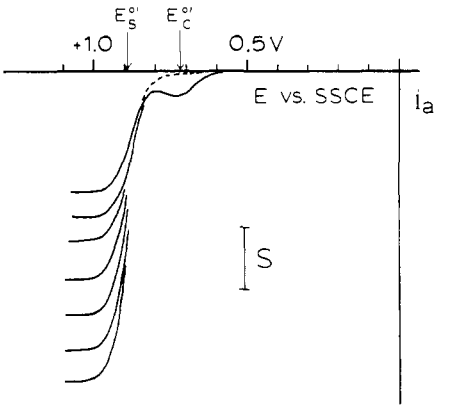

Figure 2. Rotated-disk voltammograms of a Pt/poly-$[(bpy)_2Os(vpy)_2]^{2+}$ electrode with $\Gamma_T = 6.0 \times 10^{-9}$ mol/cm^2 in a 0.49 mM $[(Me_2(bpy))_3Fe]^{2+}$ solution (0.1 M Et_4NClO_4/CH_3CN). $\nu = 10$ mV/s, $S = 45.5$ μA/cm^2, and $w = 400$, 625, 900, 1600, 2500, 3600, and 4900 rpm (top to bottom, respectively).

is seldom possible for reversible reactions) for $\Delta E°$ as large as 535 mV, and (iv) a free energy–rate correlation with the Marcus relation[10] in the thermodynamically unfavorable regime (such correlations are ordinarily done for the favored reactions[11]).

The kinetic measurements employ films of poly$[(bpy)_2Os(vpy)_2]^{2+}$ in contact with acetonitrile solutions of three series of complexes $[L_3M]^{2+}$ with M = Fe, Ru, and Os (Table I). A previous, more limited study employed films of related Ru and Fe polymers with $[L_3Ru]^{2+}$ and $[L_3Fe]^{2+}$ complexes.[12] Measurements of electron diffusion and $[L_3M]^{2+}$ permeation rates in the poly$[Os(bpy)_2(vpy)_2]^{2+}$ film are also given in order to firmly justify the assertion that eq 1 occurs exclusively at the polymer/solution interface.

Experimental Section

The $[L_3M]^{2+}$ complexes (Table I) were all synthesized as the PF_6^- salts by using standard methods.[13] The ligands 3,4,7,8-Me_4(phen), 4-Me(phen), 5-Me(phen), 4,7-Me_2(phen), 4-Ph(phen), 4,7-Ph_2(phen), 5-Cl(phen), 4,4′-Me_2(bpy), 4,4′-Ph_2(bpy), bpy, phen, 5-NO_2(phen), and 5,6-Me_2(phen), where bpy = 2,2′-bipyridine and phen = 1,10-phenanthroline, were purchased from G. F. Smith Chemicals and were used without further purification. The $[(bpy)_2Os(vpy)_2](PF_6)_2$ monomer was synthesized from $(bpy)_2OsCO_3$.[7b] All compounds were purified by column chromatography and reprecipitation.[13b] Tetraethylammonium perchlorate, Et_4NClO_4 (Eastman), was thrice recrystallized from water. Acetonitrile (Burdick and Jackson) was stored over 4-Å molecular sieves. Teflon-shrouded Pt disk electrodes were coated with poly$[(bpy)_2Os(vpy)_2]^{2+}$ by electropolymerization[4a,7] from a dilute monomer solution (0.5–0.7 mM) and stored in a desiccator before use. All experiments were performed with standard three-electrode cells and instrumentation. The total amount of polymer Γ_T (mol/cm^2) present was determined by integration of charge under the Os(II/III) cyclic voltammetric wave. The electrodes were rotated with a Model ASR2 Pine Co. RDE apparatus and steady-state kinetic currents were obtained with interrupted scans[9,12] to remove the scan-rate dependent Os(III/II) polymer wave. Microcomputer experiments were performed with a locally designed 64K unit equipped with a 50-ms IADC, two DACs, and a locally designed and constructed linear potential-ramp generator[14] with data acquisition and manipulation in BASIC.

Results

Cyclic Voltammetry of Poly$[(bpy)_2Os(vpy)_2]^{2+/3+}$. The cyclic voltammetric response of a Pt electrode coated with a film of poly$[(bpy)_2Os(vpy)_2]^{2+/3+}$ that contains 7.6×10^{-9} mol/cm^2 of Os(II) sites in 0.1 M Et_4NClO_4/CH_3CN is shown in Figure 1A. This polymer exhibits well-defined electrochemistry; at coverages and scan rates like those in Figure 1A, it displays a direct proportionality between peak current (i_p) and scan rate (v), a small peak splitting (ΔE_p), and a constant wave shape for all Os coverages examined (thicknesses ca. 70–500 Å).

Accurate analysis of the Os(III/II) wave shape was important for the electron diffusion rate measurement presented later. The ratio of $i_pRT/n^2F^2A\Gamma_T$ to scan rate is smaller (ca. 0.15 vs. 0.25) and the waves are broader (ΔE_{FWHM} = 120–140 mV vs. 90.6 mV) than expected from the simplest voltammetric theory for Nernstian reactions of surface-immobilized species.[15] The Nernstian relationship between the surface-species activity and actual (mol/cm^2) surface coverage is normally expressed with activity coefficients/interaction parameters.[9,16] Figure 1B shows a background-corrected cyclic voltammogram[17] obtained with a microcomputer electrochemistry setup for this same electrode, with a superimposed theoretical voltammogram (●●●) based on the "G" interaction parameter relation of Ikeda et al.[9] The agreement is excellent except in the most positive region (0.75–0.90 V vs. SSCE) where there is a peak for a small film impurity[9] (ca. 2–6%), which is not significant as discussed later.

Electron-Transfer Reactions of Poly$[Os(bpy)_2(vpy)_2]^{3+}$ with Solutions of $[L_3Fe]^{2+}$. Rotated-disk voltammograms for a Pt/poly-$[(bpy)_2Os(vpy)_2]^{2+}$ electrode containing $\Gamma_T = 6.0 \times 10^{-9}$ mol/cm^2 of electroactive Os sites, in a 0.49 mM solution of $[(Me_2(bpy))_3Fe]^{2+}$ (II) in 0.1 M Et_4NClO_4/CH_3CN are shown in Figure 2. Since the formal potential $E_s°'$ for II is more positive (0.89_0 V) than $E_c°'$ for the Os(II/III) reaction of the polymer (0.72_0 V), its oxidation as in eq 1 is thermodynamically unfavorable by 0.17 V. This "back reaction" nonetheless persistently occurs, driven by regeneration of Os(III) states by the electrode and by the convective removal of $[(Me_2(bpy))_3Fe]^{3+}$, and is rapid

(10) Marcus, R. A. *Annu. Rev. Phys. Chem.* **1964**, *15*, 155.
(11) Sutin, N. *Acc. Chem. Res.* **1982**, *15*, 275.
(12) Ikeda, T.; Leidner, C. R.; Murray, R. W. *J. Am. Chem. Soc.* **1981**, *103*, 7422.
(13) (a) Burstall, F. H.; Nyholm, R. S. *J. Chem. Soc.* **1952**, 3570. The low solubility of some ligands required the addition of DMF (ca. 20 vol %) to the aqueous solution. (b) Sullivan, B. P.; Salmon, D. J.; Meyer, T. J. *Inorg. Chem.* **1978**, *17*, 3334. (c) Kober, E. M.; Caspar, J. C.; Sullivan, B. P.; Meyer, T. J., manuscript in preparation.
(14) Details are available through the authors or W. S. Woodward, Electronics Consultant, Department of Chemistry, UNC-CH.
(15) Lane, R. F.; Hubbard, A. T. *J. Phys. Chem.* **1973**, *77*, 1401.
(16) (a) Brown, A. P.; Anson, F. C. *Anal. Chem.* **1977**, *49*, 1589. (b) Smith, D. F.; Willman, K. W.; Kuo, K.-N.; Murray, R. W. *J. Electroanal. Chem.* **1979**, *95*, 217.
(17) The anodic peak current is consistently ca. 10–15% smaller than the cathodic peak current, but the charge under the two waves is the same, which suggests differing activity effects for the anodic and cathodic reactions. Numerous voltammograms have been analyzed, and this subtle effect is consistently observed. The cyclic voltammogram of Pt/poly$[(bpy)_2Os(vpy)_2]^{2+/3+}$ shown is in Figure 1B accurately described with differing $G_a = -1.5$ (±0.1) and $G_c = -0.9$ (±0.1) with $E_c°' = 0.72_0$ V vs. SSCE. This interaction parameter difference is small compared to those sometimes found in uncharged, poorly swollen redox polymers.[18]
(18) Daum, P.; Murray, R. W. *J. Electroanal. Chem.* **1979**, *103*, 289.

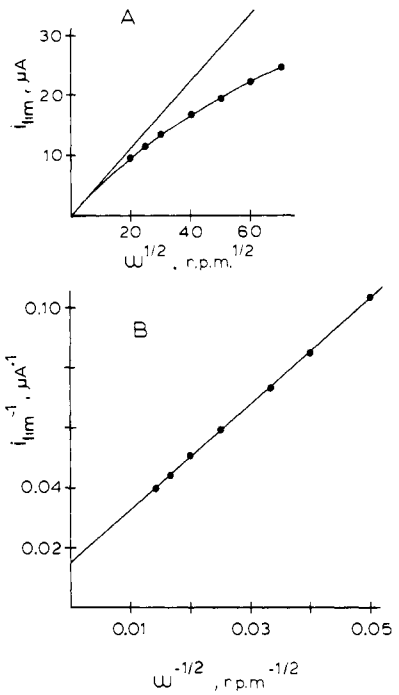

Figure 3. (A) Levich plot for i_{lim} data (●) from Figure 2. The (—) line above the data is mass-transport limited i_{lim} calculated for a bare Pt electrode of the same area. (B) Koutecky–Levich plot for this data; intercept yields $k_{12}\Gamma = 0.026$ cm/s.

enough to yield a limiting current i_{lim} at ca. 1.1 V. The i_{lim} currents do not vary proportionately with the square root of electrode rotation rate ($\omega^{1/2}$) and are less than the calculated $[L_3M]^{2+}$ mass transport i_{lim} for a bare Pt electrode (—), especially at faster rotation (Figure 3A). This is because the currents are limited by the electron-transfer rate of eq 1 as well as by mass transport. The currents are not, on the other hand, limited by electron diffusion (e.g., the supply of Os(III) sites) in the polymer film and involve negligible permeation of the substrate into the polymer film, important assertions we will justify below. The limiting currents are described by the Koutecky–Levich equation

$$(i_{lim})^{-1} = (nFAk_{12}\Gamma C_s)^{-1} + (i_{lev})^{-1} \quad (2)$$

where $i_{lev} = 0.62nFAD_s^{2/3}\nu^{-1/6}\omega^{1/2}C_s$, C_s and D_s are the substrate complex concentration (mol/cm^3) and diffusion coefficient (cm^2/s), k_{12} is the second-order electron-transfer rate constant (cm^3/(mol s), eq 1), and Γ is the quantity of Os polymer sites participating in eq 1 (less than Γ_T, vide infra). The product $k_{12}\Gamma$ is the effective heterogeneous rate constant (cm/s) of eq 1 at the polymer/solution interface and is obtained by a plot of eq 2 as in Figure 3B. The intercept of this "inverse Levich" plot yields $k_{12}\Gamma = 0.026$ cm/s for the voltammograms of Figure 2.

Seven similar experiments with $[(Me_2(bpy))_3Fe]^{2+}$ revealed analogous behavior and further showed (Table II) that $k_{12}\Gamma$ for this complex does not vary with Γ_T from 1.4 to 6.0 × 10^{-9} mol/cm^2 or with C_s from 0.5 to 1.0 mM, results consistent with assumptions inherent in eq 2 (vide infra). Accordingly, $k_{12}\Gamma$ was converted to k_{12} using $\Gamma = 10^{-10}$ mol/cm^2, approximately a monolayer of Os sites in the polymeric film based upon elementary size considerations (d = 14 Å)[19] and relative collision frequencies.[9,20]

Nine other $[L_3Fe]^{2+}$ complexes selected to have formal potentials ($E_s^{\circ\prime}$) ranging from 0.81_3 to 1.04_6 V vs. SSCE gave results parallel to the experiments in Figures 2 and 3 with rate constants as shown in Table II.[21] Expressing the driving force for the reaction of each complex in eq 1 as $\Delta E^\circ = E_s^{\circ\prime} - E_c^{\circ\prime}$ and the equilibrium constant thereby as $K_{12} = 10^{-\Delta E^\circ/0.059}$, we are able in this series to measure the back-reaction rate for reactions with $K_{12} = 7 \times 10^{-2}$ to 2×10^{-6} (Table II). Note that the ability to study such thermodynamically disfavored processes, for reversible reactions, is a result of the electrode-driven regeneration of Os(III) states at the polymer/solution interface.

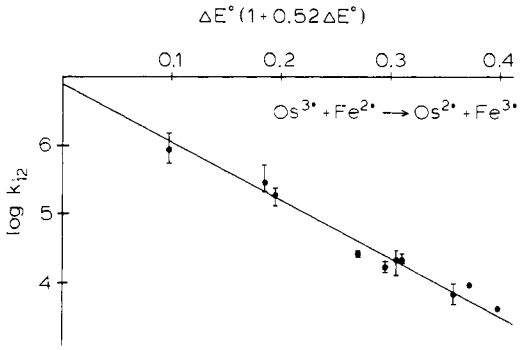

Figure 4. Plot of log (k_{12}) vs. $\Delta E^\circ(1 + X\Delta E^\circ)$ based on eq 5 for the $[L_3Fe]^{2+}$ series. Data from Table III. Error bars represent the range of data.

The electron-transfer rate constants k_{12} for reaction of the nine complexes in Table II in eq 1 decrease systematically with increasing ΔE°. Since the electron-transfer self-exchange rates k_{22} for such related $[L_3Fe]^{2+}$ complexes are nearly the same,[22] this apparent free energy–rate relationship can be examined with the Marcus equation[10] for outer-sphere electron-transfer kinetics. Neglecting work terms,[23] this is

$$k_{12} = (k_{11}k_{22}K_{12}f)^{1/2},\ \log f = (\log K_{12})^2/[4\log(k_{11}k_{22}/Z^2)] \quad (3)$$

where Z is the bimolecular collision frequency for two reactants in homogeneous solution, ca. 10^{11} M^{-1} s^{-1}, and k_{11} and k_{22} are the individual self-exchange rates for Os(III/II) and Fe(III/II).

We have chosen for reasons of convenience in comparing k_{12} to ΔE° to rearrange eq 3 into

$$\log k_{12} = 0.5\log(k_{11}k_{22}) - 8.47\Delta E^\circ(1 + X\Delta E^\circ) \quad (4)$$

where X is a function[24a] of $k_{11}k_{22}$ and is found as follows. To first approximate X and $k_{11}k_{22}$, we plot the data as log k_{12} vs. ΔE° (i.e., assume X = 0), giving a linear plot (within the scatter in the data) with slope −9.7 V^{-1} and an intercept $k_{11}k_{22} = 7.4 \times 10^{13}$ M^{-2} s^{-2}. The value of X is then calculated (gives X = 0.52), and the data are replotted as log k_{12} vs. $\Delta E^\circ(1 + X\Delta E^\circ)$ (Figure 4), using the theoretical slope[24b] of −8.47 V^{-1}. The intercept of this plot yields $k_{11}k_{22} = 6.3 \times 10^{13}$ M^{-2} s^{-2}, which again gives X = 0.52, indicating no need for further iteration.

The thus obtained value of $k_{11}k_{22} = 6.3 \times 10^{13}$ M^{-2} s^{-2} is in excellent agreement with the product, 8.1×10^{13} M^{-2} s^{-2}, of literature[22] self-exchange rates for $[(bpy)_3Fe]^{2+}$ and $[(bpy)_3Os]^{2+}$ in acetonitrile. This agreement for $k_{11}k_{22}$ indicates, in other words, that the Marcus eq 4 could be used a priori to predict, on the average, the k_{12} values of Table II to within 16% (low) of the experimental data. Considering all sources of error in the experiment/theory comparison (the value for the interfacial quantity of Os sites in the polymer (Γ), the possible variation of k_{22} within the $[L_3Fe]^{2+}$ series, and the apparent normalcy of the self-exchange rate constant k_{11} for the Os sites in the outermost polymer

(19) Since the metal–ligand bond distances for Os and Ru complexes are nearly identical (Griffith, W. P. "The Chemistry of the Rarer Platinum Metals"; Wiley: London, 1967; p 39.), the value calculated for $[(bpy)_3Ru]^{2+}$, 14 Å (Powers, M. J.; Meyer, T. J. *Inorg. Chem.* **1978**, *17*, 1785), is appropriate for $[(bpy)_2Os(vpy)_2]^{2+}$.

(20) Andrieux, C. P.; Dumas-Bouchiat, J. M.; Saveant, J.-M. *J. Electroanal. Chem.* **1981**, *123*, 171.

(21) These complexes at naked Pt all show reversible cyclic voltammetric and rotated-disk electrode electrochemistry and give formal potentials $E_s^{\circ\prime}$ (Table I) agreeing within ±5 mV.

(22) Chan, M. S.; Wahl, A. C. *J. Phys. Chem.* **1978**, *82*, 2543.

(23) Work terms, to the extent that they do not cancel (the reactions are all of the (2+,3+)/(3+,2+) type, cf.: Haim, A.; Sutin, N. *Inorg. Chem.* **1980**, *15*, 476), are expected to be constant throughout the complexes studied. The electrolyte concentration is similar to that used for the solution k_{11} and k_{22} data.[22]

(24) (a) It can be shown that $X = -1/[0.236\log(k_{11}k_{22}/Z^2)]$. (b) The least-squares slope of this data is −7.93 V^{-1}, which is only 6% low and certainly within the limits of our analysis.

Table II. Electron-Transfer Kinetics Data for Pt/Poly[$(bpy)_2Os(vpy)_2]^{3+}$ and $[L_3Fe]^{2+}$

substrate	$\Delta E^{\circ\prime}$, V	K_{12}	$10^9\Gamma_T$, mol/cm^2	C_s, mM	$k_{12}\Gamma$, cm/s	k_{12}(av),[a] M^{-1} s^{-1}
I. $[(3,4,7,8\text{-}Me_4(phen))_3Fe]^{2+}$	0.092	2.8×10^{-2}	1.6	0.131	0.15	$9 (\pm 3) \times 10^5$
			2.3	0.131	0.066	
			3.9	0.131	0.060	
			1.6	0.266	0.075	
			2.3	0.266	0.082	
			3.9	0.266	0.12	
			1.6	0.611	0.097	
			3.9	0.611	0.088	
			6.4	0.611	0.054	
II. $[(4,4'\text{-}Me_2(bpy))_3Fe]^{2+}$	0.170	1.3×10^{-3}	1.4	0.49	0.052	$2.9 (\pm 1) \times 10^5$
			6.0	0.49	0.026	
			2.4	0.61	0.026	
			3.9	0.61	0.026	
			4.5	0.61	0.024	
			4.5	0.98	0.021	
			3.8	0.98	0.027	
III. $[(4,7\text{-}Me_2(phen))_3Fe]^{2+}$	0.178	9.6×10^{-4}	1.6	0.253	0.024	$1.9 (\pm 0.6) \times 10^5$
			4.0	0.253	0.021	
			4.0	0.720	0.013	
IV. $[(4,7\text{-}Ph_2(bpy))_3Fe]^{2+}$	0.240	8.6×10^{-5}	2.65	0.290	2.9×10^{-3}	$2.7 (\pm 0.3) \times 10^4$
			3.9	0.290	2.7×10^{-3}	
			3.9	0.737	2.4×10^{-3}	
V. $[(4\text{-}Me(phen))_3Fe]^{2+}$	0.260	3.9×10^{-5}	2.6	0.300	2.1×10^{-3}	$1.7 (\pm 0.4) \times 10^4$
			6.7	0.300	1.4×10^{-3}	
			3.5	0.796	1.6×10^{-3}	
VI. $[(4,7\text{-}Ph_2(phen))_3Fe]^{2+}$	0.268	2.9×10^{-5}	2.0	0.229	3.1×10^{-3}	$2.2 (\pm 0.9) \times 10^4$
			6.1	0.229	2.3×10^{-3}	
			6.4	0.750	1.3×10^{-3}	
VII. $[(5,6\text{-}Me_2(phen))_3Fe]^{2+}$	0.272	2.5×10^{-5}	2.0	0.261	2.0×10^{-3}	$2.2 (\pm 0.4) \times 10^4$
			2.0	0.708	2.7×10^{-3}	
			6.1	0.708	1.9×10^{-3}	
VIII. $[(5\text{-}Me(phen))_3Fe]^{2+}$	0.308	6.0×10^{-6}	3.1	0.267	1.0×10^{-3}	$7.1 (\pm 2.6) \times 10^3$
			6.7	0.267	6.4×10^{-4}	
			3.1	0.840	4.9×10^{-4}	
IX. $[(bpy)_3Fe]^{2+}$	0.320	3.8×10^{-6}	2.2	1.28	10×10^{-4}	$9.6 (\pm 0.4) \times 10^3$
			4.9	1.28	9.3×10^{-4}	
X. $[(phen)_3Fe]^{2+}$	0.338	1.9×10^{-6}	2.45	1.53	4.3×10^{-4}	$4.4 (\pm 0.1) \times 10^3$
			5.5	1.53	4.4×10^{-4}	

[a] Calculated with $\Gamma = 10^{-10}$ mol/cm^2 (monolayer) from measured $k_{12}\Gamma$ values.[9,19]

monolayer), such agreement with theory is striking. The range of ΔE° and $k_{12}\Gamma$ involved in the comparison is on the other hand too large, plus the existence of other correlations below, for the agreement to be regarded as merely fortuitous.

Justification of Eq 2. Consider now the assumptions of eq 2. Our analysis takes Γ, the quantity of Os polymer sites participating in the electron-transfer mediation reaction, as ca. 10^{-10} mol/cm^2, approximately a monolayer. This can be the case if the rate of consumption of $[L_3M]^{2+}$ by Os(III) sites at the polymer/solution interface by eq 1 is faster than the rate of permeation of $[L_3M]^{2+}$ into the polymer film and is slower than the rate of resupply of Os(III) sites through the film as determined by the electron-diffusion rate in poly$[Os(bpy)_2(vpy)_2]^{2+}$.[25] The permeation rate $PD_{s,pol}$ of $[(bpy)_3Ru]^{2+}$ and presumably of similarly bulky, dicationic complexes like the $[L_3Fe]^{2+}$ series into poly$[Os(bpy)_2(vpy)_2]^{2+}$ films is $\leq 1.4 \times 10^{-12}$ cm^2/s, as measured in a later section. For a given eq 1 reaction rate, this permeability can be used in the reaction layer thickness relation of Saveant et al.,[8a] which measures substrate penetration δ into the polymer film prior to electron transfer. In our notation this equation is

$$\delta = PD_{s,pol}/(k_{12}\Gamma) \qquad (5)$$

where $PD_{s,pol}$ is the product of the $[L_3M]^{2+}$ partition coefficient into and diffusion coefficient within the polymer. Taking the slowest electron-transfer reaction in Table II (compound X, $k_{12}\Gamma = 0.00044$ cm/s), the reaction layer thickness δ is from eq 5 ≤ 0.3 Å, which is much thinner than a monolayer of polymeric Os sites (ca. 14 Å[19]). The assumption of eq 2 for negligible permeation of $[L_3M]^{2+}$ into the film for electron transfer is thus seen to be satisfied.

The electron-diffusion rate D_{ct} for the Os(III/II) mixed-valent state in poly$[Os(bpy)_2(vpy)_2]^{2+}$ is 5.4×10^{-9} cm^2/s as measured in a later section. Using an appropriate equation,[27a] we calculate that films used in Figure 2 can support a current of 195 mA/cm^2 before becoming limited by the rate of electron diffusion. This is over 270 times the Levich and measured limiting currents (0.72

(25) This justification has been addressed in several theoretical articles[8,9] and has been experimentally demonstrated in the case of several polymers.[9,12,26]

(26) Rocklin, R. D.; Murray, R. W. *J. Phys. Chem.* **1981**, *85*, 2104.

(27) (a) Current limited by D_{ct} is nFAD$_{ct}C_T/d$ where C_T is the Os site concentration in mol/cm^3 and d is film thickness in cm.[28] (b) That the calculated[27a] electron diffusion current >> than i_{lev} and i_{lim} was also used by Saveant[8c] ($i_E >> i_A, i_{k_1}$ in his notation) and by Ikeda[9] to justify use of eq 2 for a mediated electrocatalysis. According to more elaborate theory for irreversible[8a] and reversible[8c] reactions, partial rate control by electron difusion should furthermore cause Koutecky–Levich plots (i_{lim}^{-1} vs. $\omega^{-1/2}$) to be nonlinear; our data consistently provide very linear plots. Curiously, numerical calculations from the seemingly appropriate (Table III, case B, ref 8c) mixed electron-diffusion–cross-reaction rate control equation do not give a sensible analysis (usually $k\Gamma$ thus calculated is negative). The reason for this unrealistic theory/data comparison is not clear, but the observation of linear i_{lim}^{-1} – $\omega^{-1/2}$ plots and of the globally consistent pattern of eq 2 $k\Gamma$ results vs. Marcus theory and solution rates makes the absence of electron-diffusion kinetic interferences obvious.

(28) Murray, R. W. *Philos. Trans. R. Soc. London* **1981**, *302*, 253.

Table III. Electron-Transfer Kinetics Data with $[L_3Ru]^{2+}$ and $[L_3Os]^{2+}$ Complexes

substrate	$\Delta E^{\circ\prime}$, V	K_{12}	$10^9\Gamma_T$, mol/cm²	C_s, mM	$k_{12}\Gamma$, cm/s	k_{12}(av),[a] M^{-1} s^{-1}
XI, $[(3,4,7,8\text{-}Me_4(phen))_3Ru]^{2+}$	0.290	1.2×10^{-5}	1.8	0.109	2.5×10^{-3}	$2.3 (\pm 0.3) \times 10^4$
			4.8	0.109	2.4×10^{-3}	
			1.8	0.234	2.5×10^{-3}	
			4.8	0.234	1.8×10^{-3}	
XII, $[(4,4'\text{-}Me_2(bpy))_3Ru]^{2+}$	0.370	5.4×10^{-7}	2.6	0.562	2.6×10^{-4}	$2.5 (\pm 1.4) \times 10^3$
			1.3	0.99	4.9×10^{-4}	
			6.5	0.99	2.2×10^{-4}	
			1.3	2.06	1.6×10^{-4}	
			2.6	2.06	1.4×10^{-4}	
XIII, $[(bpy)_2Ru(3,4,7,8\text{-}Me_4(phen))]^{2+}$	0.460	1.6×10^{-8}	3.7	1.58	6.7×10^{-5}	$5.5 (\pm 1.4) \times 10^2$
			3.6	1.58	4.0×10^{-5}	
			3.7	3.03	5.8×10^{-5}	
XIV, $[(bpy)_3Ru]^{2+}$	0.535	8.6×10^{-10}	1.65	10.4	4.7×10^{-6}	$5.6 (\pm 1.3) \times 10^1$
			1.80	10.4	4.7×10^{-6}	
			2.0	12.8	5.8×10^{-6}	
			4.6	12.8	7.4×10^{-6}	
XVI, $[(5\text{-}Cl(phen))Os]^{2+}$	0.181	8.6×10^{-4}	1.56	0.25	0.035	$2.9 (\pm 1.6) \times 10^5$
			1.56	0.608	0.017	
			3.25	0.190	0.056	
			3.25	0.570	0.037	
			5.9	0.250	0.027	
			5.9	0.608	0.010	
			9.0	0.190	0.018	
XVII,[b] $[(5\text{-}NO_2(phen))_3Os]^{2+}$	0.188	6.5×10^{-4}	2.9	0.266	0.021	$1.6 (\pm 0.5) \times 10^5$
			2.9	0.578	0.011	
XVIII,[c] $[(3,4,7,8\text{-}Me_4(phen))_3Os]^{3+}$	0.150	2.9×10^{-3}	2.15	0.260	0.036	$3.8 (\pm 0.2) \times 10^5$
			4.6	0.260	0.040	

[a] Calculated with $\Gamma = 10^{-10}$ mol/cm² (monolayer) from measured $k_{12}\Gamma$ value.[9,19] [b] This compound exhibits irreversible (charge transfer) electrochemistry ($\Delta E_p \sim 100$ mV at 100 mV/s and $E_{1/2} = f(\omega)$). [c] $E_s^{\circ\prime}$ is more negative than $E_c^{\circ\prime}$, so this compound was run as a *reduction*; $\Delta E^\circ = E_c^{\circ\prime} - E_s^{\circ\prime}$. The $[L_3Os]^{3+}$ solution was generated by bulk electrolysis ($A = 0.42$ cm², $\omega = 2500$ rpm); resultant solution contained 0.260 mM $[L_3Os]^{3+}$ and 0.038 mM $[L_3Os]^{2+}$ calculated from $i_{lim,c}$ and $i_{lim,a}$ assuming equal diffusion coefficients.

and 0.45 mA/cm², respectively) at $\omega = 4900$ rpm, which shows that the electron diffusion assumption of eq 2 should also be satisfied.[27b]

We should emphasize that satisfying the two assumptions for eq 2 is vital to identifying the locus of the electron-transfer chemistry as the polymer/solution interface, and a careful analysis of the assumptions is required in each new polymer/solution situation. Indeed, some polymer films have, by possessing other combinations of $PD_{s,pol}$, D_{el}, and $k_{12}\Gamma$, rather freely accessible interiors,[29,30] which is desirable from the standpoint of the most effectve electrocatalysis.[8]

Reactions of Poly$[(bpy)_2Os(vpy)_2]^{3+}$ with Solutions of $[L_3Ru]^{2+}$. Additional reactions of the form of eq 1 were studied in analogous fashion with poly$[Os(bpy)_2(vpy)_2]^{3+}$ films and the four $[L_3Ru]^{2+}$ complexes (XI–XIV) listed in Table I. These complexes have very positive $E_s^{\circ\prime}$ (1.01_0–1.25_5 V vs. SSCE) relative to $E_c^{\circ\prime}$ for the Os(III/II) polymer, and so their reactions with it are thermodynamically quite unfavored and hence very slow with small equilibrium constants ($K_{12} = 1.2 \times 10^{-5}$ to 8.6×10^{-10}). Under these circumstances, it became necessary to increase the $[L_3Ru]^{2+}$ complex concentrations in order to generate currents large enough for reasonably accurate measurement in the rotated-disk experiment.[31] Kinetic results for these complexes are given in Table III.

As with the $[L_3Fe]^{2+}$ complexes, k_{12} in the $[L_3Ru]^{2+}$ series decreases with increasing ΔE° and with decreasing K_{12}. A fit of the data (-■-) to eq 4 as above is shown in Figure 5. Because of the small currents and the limited number of $[L_3Ru]^{2+}$ complexes available for study, the data fit of Figure 5 is not as good as that seen for the L_3Fe^{2+} series in Figure 4. Nonetheless, the value for $k_{11}k_{22}$ extrapolated from this data at $\Delta E^\circ = 0$, 4×10^{14} M^{-2} s^{-2}, is reasonably close to that calculated from homogenous solution self-exchange rate constants,[22] 1.8×10^{14} M^{-2} s^{-2}.

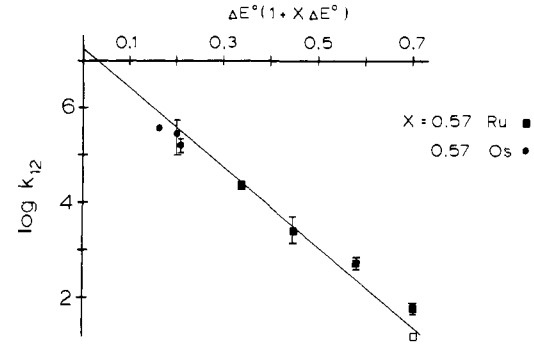

Figure 5. Plot of log (k_{12}) vs. $\Delta E^\circ(1 + X\Delta E^\circ)$ for the $[L_3Ru]^{2+}$ (-■-) and $[L_3Os]^{2+}$ (●) complexes: XVII, XV, and XVI (○) and XI, XII, XIII, and XIV (■) from left to right. k_{12} for XIV corrected for $\Gamma = 3.7 \times 10^{-10}$ mol/cm² (see text) is (□).

In the $[L_3Ru]^{2+}$ series, complex XIV, $[(bpy)_3Ru]^{2+}$, is of particular interest since its reaction in eq 1 is extraordinarily unfavored, having a $\Delta E^\circ = 535$ mV, and because its voltammogram is more complex than that in Figure 2. Figure 6A shows rotated-disk voltammograms at a series of rotation rates of a Pt/poly$[(bpy)_2Os(vpy)_2]^{3+}$ electrode with $\Gamma_T = 1.78 \times 10^{-9}$ mol/cm² in a 10.4 mM $[(bpy)_3Ru]^{2+}$ solution. The voltammogram shows three features, (a) the poly$[(bpy)_2Os(vpy)_2]^{2+/3+}$ surface wave at 0.72 V, (b) the oxidation of $[(bpy)_3Ru]^{2+}$ as in eq 1 at 1.05 V, and (c) a wave with $E_{1/2} = 1.26$ V $= E_s^{\circ\prime}$ (Table I) for direct oxidation of $[(bpy)_3Ru]^{2+}$ at the Pt electrode surface. Only

(29) (a) Anson, F. C.; Saveant, J.-M.; Shigehara, K. *J. Am. Chem. Soc.* **1983**, *105*, 1096. (b) Ohsaka, T.; Anson, F. C. *J. Phys. Chem.* **1983**, *87*, 214. (c) Anson, F. C.; Saveant, J.-M.; Shigehara, K. *J. Electroanal. Chem.* **1983**, *145*, 423. (d) Anson, F. C.; Ohsaka, T.; Saveant, J.-M. *J. Am. Chem. Soc.* **1983**, *105*, 4883.

(30) Lewis, N. S.; Bocarsly, A. B.; Wrighton, M. S. *J. Phys. Chem.* **1980**, *84*, 2033.

(31) Even so, the currents observed for complexes XIII and XIV were small and sometimes comparable in size to the background currents. Because of the small currents, the experimental uncertainty in i_{lim} is probably a factor of 2.

Table IV. Permeability of Poly[$(bpy)_2Os(vpy)_2$]$^{2+/3+}$

substrate	$10^9\Gamma_T$, mol/cm^2	C_s, mM	$PD_{s,pol}$[apparent], cm^2/s[a]
XIV	1.8	10.4	2.2×10^{-11}
	2.0	12.8	3.3×10^{-12}
	2.4	4.93	4.8×10^{-12}
	4.6	12.8	1.4×10^{-12}

[a] Calculated from eq 7 assuming $C_T = 1.5 \times 10^{-3}$ mol/cm^3. The values for XIV are upper limits due to interference by pinhole transport noticeable at the high C_s and current sensitivities employed (see text).

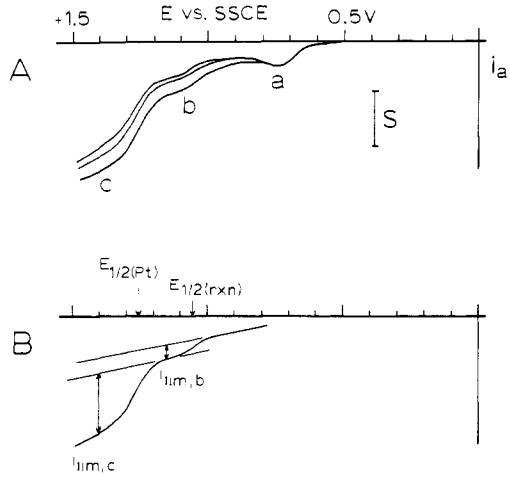

Figure 6. (A) Rotated-disk voltammograms at 400, 900, and 2500 rpm (top to bottom) for Pt/poly-$[(bpy)_2Os(vpy)_2]^{2+}$ electrode with $\Gamma_T = 1.78 \times 10^{-9}$ mol/cm^2 in a 10.4 mM $[(bpy)_3Ru]^{2+}$ solution (0.1 M Et_4ClO_4/CH_3CN). $v = 5$ mV/s and $S = 8.2$ μA/cm^2. Features a, b, and c arise from the polymer electrochemistry, eq 1, and oxidation of $[(bpy)_3Ru]^{2+}$ at underlying Pt electrode via permeation/pinholes, respectively. (B) Rotated-disk voltammogram at 900 rpm from Figure 6A with wave a removed to illustrate measurement of $i_{lim,b}$ and $i_{lim,c}$. $E_{1/2}$(rxn) and $E_{1/2}$(Pt) are $E_{1/2}$ of waves b and c.

waves b and c appear in Figure 6B, which was determined point by point so as to yield true steady-state currents and cause wave a, the Os(III/II) polymer wave, to disappear. $k_{12}\Gamma$ was obtained from $i_{lim,b}$ with eq 2. Over the investigated range of electrode rotation rate, $i_{lim,b}$ varied at most 10% and for most electrodes not at all.

The assignment of the limiting current $i_{lim,b}$ to the electron-transfer reaction eq 1 is supported by similarity of the $E_{1/2}$ for wave b, 1.05 V in Figure 6B, to the theoretical half-wave potential, $E_{1/2,rxn} = 1.07$ V, calculated[8a,9] for this situation from the equation

$$E_{1/2,rxn} = E_s^{\circ\prime} + (RT/nF) \ln (i_{lim,b}/i_{lev}) \quad (6)$$

where i_{lev} (vide supra) is the limiting current for oxidation of $[L_3Ru]^{2+}$ at a bare Pt electrode.

Measuring the rate of oxidation of $[(bpy)_3Ru]^{2+}$ in eq 1 exemplifies the potency of the rotated-disk experiment to directly study back-reaction rates. For the experiment in Figure 6B, one can calculate from $i_{lim,b}$ that each Os(III) site at the polymer/solution interface accepts, on the average, an electron from a $[(bpy)_3Ru]^{2+}$ complex only once each 5 s. For $[(bpy)_3Ru]^{2+}$, ΔE° is 535 mV and K_{12} is only 8.6×10^{-10}. Under the conditions of Figure 6B, this means that, were eq 1 allowed to come to equilibrium, only ca. 3×10^{-6} M Os(II) sites and $[L_3Ru]^{3+}$ would exist at the polymer/solution interface. Besides the electrode-driven rapid consumption of the Os(II) states and the hydrodynamic removal of $[L_3Ru]^{3+}$, a key advantageous factor is the high concentration of Os(III) sites in the polymer, ca. 1.5 M.

Permeability of Poly[$(bpy)_2Os(vpy)_2$]$^{2+/3+}$ Film to $[(bpy)_3Ru]^{2+}$. Wave c in Figure 6B is identified from equality of its $E_{1/2}$ to $E_s^{\circ\prime}$ for $[(bpy)_3Ru]^{2+}$ to be due to oxidation of $[(bpy)_3Ru]^{2+}$ at the polymer film/Pt electrode interface. This was an important observation, permitting estimation of an upper limit for the polymer film permeability $Pd_{s,pol}$ as follows. First assume control of wave c by permeation of the complex through the polymer and that there is negligible current due to transport of complex through pinholes in the film. Further assume the simple equation for one-wave voltammograms[32]

$$[i_{lim,c}]^{-1} = [nFAPD_{s,pol}C_s/d]^{-1} + [i_{lev}]^{-1} \quad (7)$$

where d is film thickness calculated from Γ_T/C_T with C_T being Os polymer site concentration estimated as 1.5×10^{-3} mol/cm^3 by analogy with poly[$Ru(vbpy)_3$]$^{2+}$.

As shown in Table IV, the apparent $PD_{s,pol}$ thus measured from $i_{lim,c}$ decreases as the film thickness increases. This trend is not expected[33] for a straightforward permeation process and is interpreted in terms of film imperfections and pinholes, whose incidence is greatest with the thinnest film studied (that in Figure 6B) and less (but not altogether absent, vide infra) at larger thicknesses. Given the high current sensitivity and high concentration C_s, only a small incidence of pinholes is required to produce these effects, and Figure 6B is the "worst-case" voltammogram observed for XIV (thinnest Os film studied). (Also, use of more rigorous, but more complex, "(S + R)" two-wave voltammogram relations[8a] instead of eq 7 was consequently thought not warranted.)

The data in Table IV show that $PD_{S,pol}$ can be no greater than ca. 1.4×10^{-12} cm^2/s for $[(bpy)_3Ru]^{2+}$ in the Os polymer film. If eq 5 is now applied using $PD_{s,pol} \leq 1.4 \times 10^{-12}$ cm^2/s and $k_{12}\Gamma = 5.6 \times 10^{-6}$ cm/s measured for $[(bpy)_3Ru]^{2+}$, we obtain $\delta \leq 25$ Å. This is more than a monolayer dimension and (by itself) implies that the reaction zone in eq 1 for the case of $[(bpy)_3Ru]^{2+}$ (XIV) includes the outermost two–four monolayers of polymeric Os sites, not just the outermost single monolayer. However, keep in mind that the $PD_{s,pol}$ used is an upper limit, and note the contradiction arising, that $\delta < 25$ Å is ca. 10 times *less* than the thickness (ca. 307 Å) of the $\Gamma_T = 4.6 \times 10^{-9}$ mol/cm^2 film which gave the $PD_{s,pol}$ estimate. The contradiction is that all of the $[(bpy)_3Ru]^{2+}$ should be consumed within the outer ca. 10% of the film thickness, i.e., that wave c for oxidation of $[(bpy)_3Ru]^{2+}$ at the Pt electrode should not be observable. The contradiction is resolved if we recognize that the wave c currents are mainly supplied by diffusion of $[(bpy)_3Ru]^{2+}$ through pinholes in the film, so that $\delta \leq 25$ Å is, consequently, an overestimate of δ. The $[(bpy)_3Ru]^{2+}$ is probably consumed at shorter and perhaps monolayer distances. The lower, right-hand point in Figure 5 for $[(bpy)_3Ru]^{2+}$ is ■ assuming a monolayer reaction, □ assuming $\delta = 25$ Å.

Complex XIV was the only complex in this study for which film permeability was an issue. For the other complexes, estimates of a reaction layer thickness δ, calculated by eq 5 and the $PD_{s,pol}$ upper limit, indicated that no more than a monolayer value of Os sites would react in eq 1. Also, importantly, the other complexes did not display waves like wave c of Figure 6.

Reactions of Pt/Poly[$(bpy)_2Os(vpy)_2$]$^{2+}$ with Solutions of $[L_3Os]^{2+}$ Complexes. Eq 1 rate measurements were also conducted for three $[L_3Os]^{2+}$ complexes (XVI–XVIII, Table I). Compound XVII, unexpectedly and unlike the other $[L_3M]^{2+}$ complexes in Table I, showed (charge-transfer) irreversible electrochemistry at bare Pt; its ΔE_p was 100 mV at 100 mV/s in cyclic voltammetry and rotated-disk $E_{1/2}$ potentials increased with rotation rate. This is possibly the reason $k_{12}\Gamma$ for XVII is smaller (Table III) by ca. 2 times than $k_{12}\Gamma$ for XVI, which has a similar ΔE° (0.18_1 vs. 0.18_8 V).

(32) (a) Schmehl, R. H.; Murray, R. W. *J. Electroanal. Chem.* **1983**, *152*, 97. (b) Ikeda, T.; Schmehl, R. H.; Denisevich, P.; Willman, K. W.; Murray, R. W. *J. Am. Chem. Soc.* **1982**, *104*, 2683.

(33) The *relative* contribution of currents due to reactants diffusing through film imperfections and pinholes, to react at the underlying electrode, increases when the rate of permeation $PD_{s,pol}$ of the reactant through the polymer phase itself is smaller. In our previous work[32] on permeation, we did not observe variations in $PD_{s,pol}$ with Γ_T like those shown in Table IV; $PD_{s,pol}$ was relatively constant. That work dealt with more rapid permeants, and the conclusions reached there about the relative unimportance of pinhole effects still seem valid. Also, much lower permeant concentrations (0.1–0.2 mM) were required to give measureable currents as compared to those (10 mM) for the present case ($[Ru(bpy)_3]^{2+}$).

$$Pt/poly[(bpy)_2Os(vpy)_2]^{+2} + [L_3Os]^{3+} \xrightarrow{k_{12}} Pt/poly[(bpy)_2Os(vpy)_2]^{3+} + [L_3Os]^{2+} \quad (8)$$

$$+e^-$$

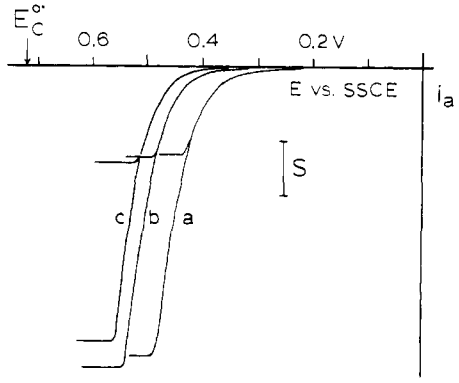

Figure 7. Rotated-disk voltammograms of Pt/poly-$[(bpy)_2Os(vpy)_2]^{2+}$ electrodes with $\Gamma_T = 1.33 \times 10^{-9}$ (a), 3.7×10^{-9} (b), and 8.3×10^{-9} mol/cm^2 (c) in 1.09 mM $[(bpy)_2OsCl_2]$, 0.1 M Et_4NClO_4/CH_3CN. ω = 400, 4900 (a); 400, 4900 (b); 400, 3600 rpm (c). v = 5 mV/s for a and 2 mV/s for b and c; S = 69.4, 68.5, and 60.1 μA/cm^2, respectively.

Complexes XVI and XVII have $E_s°'$ more positive than $E_c°'$ for poly$[(bpy)_2Os(vpy)_2]^{2+}$ and so were studied as oxidations as in eq 1. $E_s°'$ for compound XVIII is on the other hand *less positive* (Table I) than $E_c°'$; so for it, eq 1 was studied in the *reduction* direction, eq 8. The measured rate for XVIII, $k_{12}\Gamma = 0.038$ cm/s (Table III), is consistent with that for XVI and XVII. This agreement is helpful by showing that the minor poly$[Os(bpy)_2(vpy)_2]^{+2}$ film impurity we mentioned in connection with Figure 1B must be relatively unreactive.[34]

The $\Delta E°$ for the three Os/Os reactions are not sufficiently different to fit eq 4 to the k_{12} data (Table III) as was done above. Figure 5 shows, however, that they fall reasonably well (●) on the same plot as for the $[L_3Ru]^{2+}$ complexes. The $\Delta E° = 0$ intercept of this plot gave $k_{11}k_{22} = 4 \times 10^{14}$ M^{-2} s^{-2}. The literature $k_{11}k_{22}$ product for the Os/Os reaction, 4.8×10^{14} M^{-2} s^{-2}, obtained by squaring the self-exchange rate for $[(bpy)_3Os]^{2+}$ in CH_3CN, $(2.2 \pm 1.1) \times 10^7$ M^{-1} s^{-1},[22] agrees quite well with this estimate.

Electron Diffusion Rates in Poly$[(bpy)_2Os(vpy)_2]^{2+/3+}$ Films. As noted above, to justify use of eq 2, the rate D_{ct} of electron diffusion in the polymer must be sufficiently fast to avoid any depletion of Os(III) sites at the polymer/solution interface. D_{ct} for poly$[(bpy)_2Os(vpy)_2]^{2+}$ was measured using a procedure described by Ikeda,[9] observing currents due to the oxidation of $[Os(bpy)_2Cl_2]$ in eq 1. Given that $\Delta E° = -0.78$ V, according to Figure 5, $k_{12}\Gamma$ for this complex should be ca. 9×10^3 cm/s, which is ca. 10^5 times too fast to limit the rotating-disk electrode currents. Instead, rate control of the currents shifts to electron diffusion within the polymer and/or mass transport of the complex in the solution.[9]

The rotated-disk voltammograms of three different Pt/poly-$[(bpy)_2Os(vpy)_2]^{2+}$ electrodes with three different film coverages Γ_T in a 1.05 mM $[(bpy)_2OsCl_2]$ solution are shown in Figure 7.[35] The oxidation waves have a very distinctive shape,[9] in which the rising part of the wave is D_{ct} limited, and the abruptly attained plateau current is mass-transport limited (i_{lev}). The shape of the rising part of the wave is governed by the potential dependency of generating Os(III) sites at the electrode/polymer interface. Because the potential of the waves is more negative than $E_c°'$,

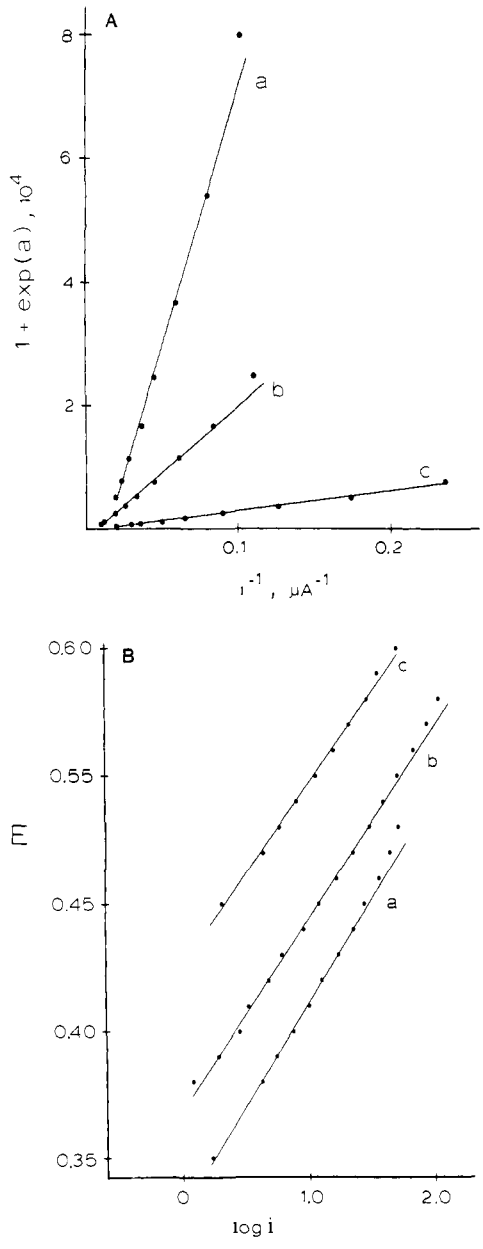

Figure 8. (A) Plot of rising part of waves in Figure 7 according to eq 20 of ref 9; $\exp(a) = \exp[(nF/RT)(E°' - E) + [(1 - 2C_{ox}/C_T)G]/2]$. (B) Plot of rising part of waves in Figure 7 according to eq 9 and 10.

the concentration of the generated Os(III) sites is quite small and they form a shallow and current-limiting $dC_{Os(III)}/dx$ gradient between the electrode/polymer and polymer/solution interfaces. The current flowing under this circumstance is given by

$$i = nFAD_{ct}C_T^2(C_{Os(III)}/C_T)/\Gamma_T \quad (9)$$

where $C_{Os(II)}/C_T$ depends on electrode potential. Eq 9 is the same as eq 20 of ref 9, which uses the "G" interaction parameter to describe how $C_{Os(III)}/C_T$ varies with potential. Plotting currents on the rising part of the waves according to that equation gives linear plots (Figure 8A) and values of D_{ct} designed as "Method

(34) Since $\Delta E°$ is smaller for the possible oxidation of complexes XVI and XVII (and the others in Table I) by the impurity state than for oxidation by the principal poly$[Os(bpy)_2(vpy)_2]^{3+}$ component, the impurity might react more rapidly and contribute to the observed current. The reverse is true on the other hand for the reduction of XVIII. The agreement of the rate $k_{12}\Gamma$ for complex XVIII with the others indicates that the impurity is relatively unreactive. Note that this could be so merely by the impurity *not* being predominantly located at the polymer/solution interface.

(35) The film coverages are such that $[(bpy)_2OsCl_2]$ permeation currents, starting at ca. −0.1 V, are significant on the scale of Figure 7a.

Table V. Charge Transport Rates in Poly$[(bpy)_2Os(vpy)_2]^{2+/3+}$

	method I[a]		method II[b]		
$10^9\Gamma_T$, mol/cm^2	$D_{ct}C_T^2/\Gamma_T$, mol/(cm^2 s)	$D_{ct}^{1/2}C_T$,[c] mol/(cm^2 s$^{1/2}$)	g	$D_{ct}C_T^2/\Gamma_T$, mol/(cm^2 s)	$D_{ct}^{1/2}C_T$,[c] mol/(cm^2 s$^{1/2}$)
1.33	1.22×10^{-5}	1.3×10^{-7}	0.72	8.5×10^{-6}	1.1×10^{-7}
3.7	1.53×10^{-5}	2.4×10^{-7}	0.78	3.0×10^{-6}	1.1×10^{-7}
8.3	4.4×10^{-6}	1.9×10^{-7}	0.81	1.4×10^{-6}	1.1×10^{-7}

[a] From eq 9 with $G_a = -1.6$; see Figure 8A. [b] From eq 9 and 10; see Figure 8B. [c] Compare with value obtained in steady-state measurement (using a Pt/poly$[(bpy)_2Os(vpy)_2]^{2+/3+}$/Au electrode configuration) of $1.1 (\pm 0.3) \times 10^{-7}$ mol/(cm^2 s$^{1/2}$).[37]

I" in Table V. We have found[4e] that the interaction parameter expression of Albery et al.[36]

$$C_{Os(III)}/C_T = [1 + \exp((gnF/RT)(E_c^{\circ\prime} - E))]^{-1} \quad (10)$$

is both simpler and more accurate for describing $C_{Os(III)}/C_T$ variation with potential at potentials far removed from $E_c^{\circ\prime}$ as in the present case. Plots of the waves of Figure 7A according to eq 9 and 10 are shown in Figure 8B and give the "Method II" results in Table V. The results from the two methods are not widely different, but that using eq 10 agrees more closely with an independent measurement of D_{ct} for this polymer with a sandwich electrode arrangement[37] ($D_{ct} = 5.4 \times 10^{-9}$ cm^2/s).

Discussion

It is rare that the locale of a chemical reaction can be quantitatively assigned to a polymer/solution interface as opposed to assuming that it occurs there. The above analysis of the assumptions involved in eq 2 showed that, except possibly for complex XIV, its assumptions were satisfied for the electron-transfer reactions studied here. That is, the analysis showed that the electron-transfer reactions occur exclusively with the outermost monolayer of poly$[(byp)_2Os(vpy)_2]^{3+}$ sites, which amounts to reaction at the polymer/solution interface. It is worth emphasizing that appropriateness of eq 2 depends on the numerical values of permeability and of electron diffusion rates for the particular system under study, and so the reader should not generalize the present conclusion to other redox polymer/metal complex reactions.

It seems reasonable to suppose that the interfacial character of eq 1 has the consequence of greatly simplifying the reaction energetics. That is, the potentially larger barriers associated with penetration and diffusion of $[(bpy)_3M]^{2+}$ complexes into the polymer film, and of electron diffusion within the film, are of no consequence. It appears in fact that the energetics of eq 1 are nearly identical with those for electron-transfer reactions between $[(bpy)_3M]^{2+}$ and $[(bpy)_3Os]^{3+}$ complexes dissolved in acetonitrile solution. The correlation between the experimental rates and the Marcus cross-electron transfer eq 4 not only shows that the rates k_{12} vary with reaction free energy (e.g., ΔE°), as prescribed by eq 4, but also the $\Delta E^\circ = 0$ extrapolated values of $k_{11}k_{22}$ agree quite well with $k_{11}k_{22}$ products calculated from independently measured self-exchange rates for dissolved complexes. This means that eq 4 could have been used a priori to calculate the rates of the eq 1 electron-transfer mediation reactions.

To summarize the correlation between $k_{11}k_{22}$ values, the experimental vs. literature products[22] for the five series of reactions studied here and earlier[12] are (Os/Fe) 6.3×10^{13} vs. 8.1×10^{13}, (Os/Ru) 4×10^{14} vs. 1.8×10^{14}, (Os/Os) 4×10^{14} vs. 4.8×10^{14}, (Ru/Ru)[12] 6.5×10^{13} vs. 6.9×10^{13}, and (Fe/Fe)[12] 4×10^{12} vs. 14×10^{12} M^{-2} s^{-2}, respectively. The agreement occurs over a 100-fold range of the observed $k_{12}k_{22}$ product.

The $k_{11}k_{22}$ comparison additionally suggests that the self-exchange rate k_{11} for poly$[(bpy)_2Os(vpy)_2]^{2+/3+}$ sites at the polymer surface is the same as that in homogeneous solution[22] for $[(bpy)_3Os]^{2+/3+}$. This is interesting and is also the first measurement of the electron-transfer rate in these polymers that is not derived from the electron diffusion rate parameter D_{ct}. The value of D_{ct} is not necessarily determined by this value of k_{11}, however, since k_{11} was derived from the behavior of polymer *surface* poly$[(bpy)_2Os(vpy)_2]^{3+}$ sites only, whereas D_{ct} measures electron hopping between *interior* sites. The energetics for electron self-exchange between Os(II) and Os(III) sites in the interior of the polymer might well additionally involve precursor motions of the polymeric framework or reflect possible differences in the internal acetonitrile solvent. To examine this point, we have calculated[37] a value of k_{11}(interior) from D_{ct} in a manner done for a related Ru-based polymer.[7a,38] The calculation takes D_{ct} as reflecting the incidence of *fruitful* collisions in a diffusion-controlled reaction and thus invokes the Smoluchowski equation where D_{ct} is the electron-diffusion coefficient (5×10^{-9} cm^2/s for poly$[(bpy)_2Os(vpy)_2]^{2+}$), and the collisional radius is 7 Å. The resulting k_{11}(interior) = 1.1×10^7 M^{-1} s^{-1} agrees rather well with the homogeneous value, 2.2×10^7 M^{-1} s^{-1}.

Electron-transfer reactions that have highly favorable free energy changes so that their rates become diffusion controlled or fall into the so-called "inverted region"[39] are of considerable interest. Experimental investigations of such reactions are conventionally carried out for the forward reaction rate because of the difficulty of measuring very slow back reactions of reversible processes (as opposed to irreversible processes which have been studied[40]). The experimental approach for the back-reaction rate k_{12} described here allows consideration of investigating fast forward rates k_{21} through the equilibrium constant connection $K_{12} = k_{12}/k_{21}$. In order to encounter effects on the back-reaction rate k_{12} from diffusional-controlled forward reactions (e.g., k_{21} = ca. 1×10^{10} M^{-1} s^{-1}), with a value of $K_{12} = 10^{-9}$, for example, one must measure a k_{12} in the range of 10 M^{-1} s^{-1}. For the complex XIV in fact we are close to this requirement, and k_{21} calculated for this complex in eq 1 is 6.5×10^{10} M^{-1} s^{-1}. The rate for XIV represented the experimental limit of our rotated-disk method as practiced here, however, and so this interesting question could not be further explored. We are hopeful that another electrochemical method can be induced to provide data for very slow eq 1 reactions but also point out that to maintain the usefulness of eq 2, complex-polymer combinations involving permeabilities as small or smaller than assessed here for poly$[(bpy)_2Os(vpy)_2]^{2+}$ must be identified.

Finally we address the relevance of this study to electrocatalysis and to existing theories. Clearly these chemical systems are excellent models to study electron transfers between polymer films and solution complexes. The reactions here are, however, not, strictly speaking, catalytic, even though as is evident from Figure 6 the voltammetric wave for the oxidation of $[Ru(bpy)_3]^{2+}$ by poly$[(bpy)_2Os(vpy)_2]^{3+}$ occurs at a potential considerably less positive than $E_s^{\circ\prime}$ of the complex. The currents flowing due to eq 1, i_{lim}, are always lower than those for the reversible oxidation of the solution complexes at bare Pt; in Figure 6, for example, i_{lim}/i_{lev} is only 8×10^{-5}. That current catalysis does not occur

(36) Albery, W. J.; Boutelle, M. G.; Colby, P. J.; Hillman, A. R. *J. Electroanal. Chem.* **1982**, *133*, 135.

(37) Pickup, P. G.; Kutner, W.; Leidner, C. R.; Murray, R. W., *J. Am. Chem. Soc.*, in press.

(38) In ref 7a, the calculated value of k_{11}(interior) (called k_{ex}^{app} there) should be correctly 4.5×10^5, not 2.3×10^5 M^{-1} s^{-1} as given there.

(39) (a) Engleman, R.; Jortner, J. *J. Mol. Phys.* **1970**, *18*, 145. (b) Freed, K. F.; Jortner, J. *J. Chem. Phys.* **1970**, *52*, 6272.

(40) (a) Andrieux, C. P.; Blocman, C.; Dumas-Bouchiat, J. M.; Saveant, J.-M. *J. Am. Chem. Soc.* **1979**, *101*, 3431. (b) Andrieux, C. P.; Blocman, C.; Dumas-Bouchiat, J. M.; M'Halla, F.; Saveant, J.-M. *Ibid.* **1982**, *102*, 3806.

in mediation reaction like eq 1 when the reaction substrate already posesses fast heterogeneous rates and the reaction occurs at a polymeric monolayer has been anticipated by theory.[20]

Acknowledgment. This work was supported by a grant from the National Science Foundation. Helpful discussions with Drs. P. G. Pickup and B. P. Sullivan and Professor T. J. Meyer are gratefully acknowledged. Assistance with electronics from W. S. Woodward is also appreciated.

Registry No. I, 88000-69-5; II, 85185-57-5; III, 88000-70-8; IV, 88000-71-9; V, 88000-72-0; VI, 88000-73-1; VII, 85202-31-9; VIII, 88000-74-2; IX, 70811-29-9; X, 17112-07-1; XI, 88000-75-3; XII, 83605-44-1; XIII, 88000-77-5; XIV, 60804-74-2; XV, 15702-72-4; XVI, 88000-78-6; XVII, 88015-26-3; XVIII, 88000-80-0; poly-$[(bpy)_2Os(vpy)_2]^{3+}$, 88080-24-4; poly-$[(bpy)_2Os(vpy)_2]^{2+}$, 88080-25-5; Pt, 7440-06-4.

Photoassisted Catalytic Oxidation of Isopropyl Alcohol by Uranyl-Exchanged Zeolites

Steven L. Suib,* Athanasios Kostapapas, and Dimitrios Psaras

Contribution from the Department of Chemistry and Institute of Materials Science, University of Connecticut, Storrs, Connecticut 06268. *Received August 19, 1983*

Abstract: Suspensions of uranyl-exchanged zeolites mixed with solutions of isopropyl alcohol and acetonitrile undergo selective photocatalytic conversion of the alcohol to acetone. The photoassisted catalytic oxidation is sustained for over 300 h. Bulk photolysis experiments show that aging does occur. X-ray photoelectron spectroscopy experiments indicate that uranyl ions on the surface are slighly reduced with respect to the bulk. Luminescence lifetime measurements yield a range of long-lived components between 10 and 700 μs for the different zeolites. Quenching experiments show that the shortest lived components of crystalline uranyl-exchanged zeolites are responsible for this conversion to acetone. Liquid nitrogen and liquid helium temperature luminescence emission spectra show splittings of the vibrational rotational fine structure as the temperature is diminished. These splittings are indicative of site symmetry, and in the case of the uranyl-exchanged HZSM-5 with the isopropyl alcohol mixture, evidence is presented that the isopropyl alcohol binds to the excited uranyl ion. The nature of the active site and factors that are important in the mechanism of this reaction are described.

Introduction

Zeolites have received much attention recently in a wide range of contexts,[1] particularly in the area of catalysis. Their catalytic and absorptive properties, primarily in the cracking of petroleum,[2] as builders in detergents,[3] and as Fischer–Tropsch catalysts,[4] have been investigated in great detail. A large effort in related areas involving spectroscopic studies of zeolites including magic angle spinning nuclear magnetic resonance,[5] X-ray diffraction,[6] surface analysis,[7] and X-ray absorption[8] has brought about several fundamental questions regarding the structure and stability of these materials.

The role of light in the transformation of reagents inside zeolites and the use of photochemical techniques, such as luminescence methods[11,13] and photoacoustic spectroscopy,[12] are resonably well understood although the number of photochemical studies of zeolites falls far behind the enormous volumes concerning thermal activation.[9,10]

Some of the most interesting and promising reports concerning the photochemical behavior of inorganic species in zeolites have been the water-splitting studies by europium,[14] silver,[15] and titanium-exchanged zeolites,[16] as well as by $Ru(bpy)_3^{2+}$ complexes in zeolites.[17] Electron-transfer[12,18] and energy-transfer[19] reactions have also been reported recently. Further discussion of these studies can be found elsewhere.[20]

Since this time, work by Lunsford and Camera[21] has shown that infrared spectroscopy can be used to explore the photoaquation of transition metal complexes like iodopentaamminerhodium(III). Valuable information regarding quantum yields and scattering was obtained. Ammonia has also been photogenerated over zeolites.[22]

(1) (a) Maxwell, I. A. *Adv. Catal.* **1982**, *31*, 1–76. (b) Naccache, C. *J. Phys. Chem.* **1983**, *87*, 2175–2179.
(2) Chen, N. Y. U. S. Patent 3630966, 1971.
(3) *Chem. Eng. News* **1982**, *60*(39), 10–15.
(4) (a) Chang, C. D.; Lang, W. H.; Silvestri, A. J. *J. Catal.* **1979**, *56*; 268–273. (b) Caesar, P. D.; Brennan, J. A.; Garwood, W. E.; Ciric, J. *Ibid.* **1979**, *56*, 274–278. (c) Nijs, H. H.; Jacobs, P. A.; Uytterhoeven, J. B. *J. Chem. Soc., Chem. Commun.* **1979**, 180–181. (d) Haag, W. O.; Huang, J. J. U. S. Patent 9157338, 1979.
(5) (a) Klinowski, J.; Thomas, J. M.; Audier, M.; Vasudevin, S.; Fyfe, C. A.; Hartman, J. S. *J. Chem. Soc., Chem. Commun.* **1981**, 570–571. (b) Engelhardt, G.; Lippmaa, E.; Magi, M. *Ibid.* **1981**, 712–713.
(6) (a) Pluth, J. J.; Smith, J. V. *J. Am. Chem. Soc.* **1983**, *105*, 2621–2624. (b) Gellens, L. R.; Smith, J. V.; Pluth, J. J. *Ibid.* **1983**, *105*, 51–55.
(7) (a) Derouane, E. G.; Gilson, J. P.; Gabelica, F.; Mousty-Desbuquoit, C.; Verbist, J. *J. Catal.* **1980**, *71*, 447–448. (b) Dwyer, J.; Fitch, F. R.; Machado, F.; Qin, G.; Smyth, S. M.; Vickerman, J. C. *J. Chem. Soc., Chem. Commun.* **1981**, 422–423. (c) Suib, S. L.; Coughlin, D. F.; Otter, F. A.; Conopask, L. *J. Catal.*, in press.
(8) (a) Morrison, T. I.; Reis, A. H.; Gerbert, E.; Iton, L. E.; Stucky, G. D.; Suib, S. L. *J. Chem. Phys.* **1980**, *72*, 2676–2682. (b) Morrison, T. I.; Iton, L. E., Shenoy, G. K.; Stucky, G. D.; Suib, S. L.; Reis, A. H. *Ibid.* **1981**, *73*, 4705–4706. (c) *Chem. Eng. News* **1981**, *59*(15), 32
(9) Fraenkel, D.; Gates, B. C. *J. Am. Chem. Soc.* **1980**, *102*, 2478–2480.
(10) (a) Scherzer, J.; Fort, D. *J. Catal.* **1981**, *71*, 111–118. (b) Suib, S. L.; McMahon, K. C.; Psaras, D. In "Intrazeolite Chemistry", Stucky G. D., Dwyer, F. G., Eds.; American Chemical Society: Washington, D.C., 1983 pp 301–318; *ACS Symp. Ser.* No 218.
(11) Arakawa, T.; Takata, T.; Adachi, G. Y.; Shiokawa, J. *J. Chem. Soc., Chem. Commun.* **1979**, 453–454.
(12) Faulkner, L. R., Suib, S. L.; Renschler, C. L.; Green, J. M.; Bross, P. R. In "Chemistry in Energy Production"; Wymer, R. G., Keller, O. L., Eds.; Conf. 801226, 1982; pp 99–114.
(13) Pott, G. T.; Stork, W. H. *J. Catal. Rev.* **1975**, *12*, 163–199.
(14) (a) Arakawa, T.; Takata, T.; Adachi, G. Y.; Shiokawa, J. *J. Lumin.* **1979**, *20*, 325–327. (b) Suib, S. L.; Zerger, R. P.; Stucky, G. D.; Emberson, R. M.; Debrunner, R. G.; Iton, L. E. *Inorg. Chem.* **1980**, *19*, 1858–1862.
(15) Jacobs, P. A.; Uytterhoeven, J. B.; Beyer, H. K. *J. Chem. Soc., Chem. Commun.* **1977**, 128–129.
(16) (a) Kuznicki, S. M.; Eyring, E. M. *J. Am. Chem. Soc.* **1978**, *100*, 6790–6791. (b) Kuznicki, S. M.; DeVries, K. L.; Eyring, E. M. *J. Phys. Chem.* **1980**, *84*, 535–537.
(17) (a) DeWilde, W.; Peeters, G.; Lunsford, J. H. *J. Phys. Chem.* **1980**, *84*, 2306–2310. (b) Quayle, W. H.; Lunsford, J. H. *Inorg. Chem.* **1982**, *21*, 97–103.
(18) Faulkner, L. R.; Suib, S. L.; Renschler, C. L.; Green, J. M.; Bross, P. R., manuscript in preparation.
(19) Strome, D. H.; Klier, K. In "Adsorption and Ion Exchange with Synthetic Zeolites"; Flank, W. H., Ed., American Chemical Society: Washington, D.C., 1980; pp 155–176; *ACS Symp. Ser. No.* 135.
(20) Suib, S. L.; Bordeianu, O. G.; McMahon, R. C.; Psaras, D. In "Inorganic Reactions in Organized Media"; Holt, S. L., Ed.; American Chemical Society: Washington, D.C., 1981; pp 225–238; *ACS Symp. Ser. No.* 177.
(21) (a) Camara, M. J.; Lunsford, J. H. *Inorg. Chem.* **1983**, *22*, 2498–2501. (b) Camara, M. J.; Lunsford, J. H. "Abstracts of Paper", 184th National Meeting of the American Chemical Society, Kanasas City, MO, Sept 1982; American Chemical Society: Washington, D.C., 1983.

0002-7863/84/1506-1614$01.50/0